Zeno and Anti-Zeno Polarization Control of Spin Ensembles by Induced Dephasing

Gonzalo A. Álvarez,[1,2] D. D. Bhaktavatsala Rao,[3] Lucio Frydman,[3,*] and Gershon Kurizki[3,†]

[1]*Facultad de Matemática, Astronomía y Física, Universidad Nacional de Córdoba, 5000 Córdoba, Argentina*
[2]*Fakultät Physik, Universität Dortmund, Otto-Hahn-Strasse 4, D-44221 Dortmund, Germany*
[3]*Department of Chemical Physics, Weizmann Institute of Science, Rehovot, 76100, Israel*

We experimentally and theoretically demonstrate the purity (polarization) control of qubits entangled with multiple spins, using induced dephasing in nuclear magnetic resonance setups to simulate repeated quantum measurements. We show that one may steer the qubit ensemble towards a quasiequilibrium state of a certain purity by choosing suitable time intervals between dephasing operations. These results demonstrate that repeated dephasing at intervals associated with the anti-Zeno regime leads to ensemble purification, whereas those associated with the Zeno regime lead to ensemble mixing.

Introduction.—The ability to understand and manipulate the dynamics of "open" quantum systems, i.e., systems that interact with their environment, is a challenge for fundamental quantum physics and a prerequisite for applications such as quantum heat engines [1], quantum information storage and retrieval [2], and precision measurements [3]. This is particularly true for spin-1/2 particles (qubits); systems that are usually controllable by coherent fields [4,5]. Here we address their manipulations by incoherent, random fields mimicking quantum nondemolition (QND) measurements [6,7]. Such manipulations are intriguing: whereas QND measurements leave a closed system intact, they can affect an open system by destroying its correlations (coherences) with the bath. As recently predicted for qubits coupled to thermal oscillator baths, such measurements can steer the qubit ensemble towards either higher or lower purity ("cooling" or "heating") [8]; the qubit does not retain its state as the measurements accumulate, but rather converges to an asymptotic steady state. In the quantum Zeno (QZE) regime, frequent measurements can raise the asymptotic excitation (and entropy) of the qubit. This reflects the hitherto unnoticed fact that QZE dynamics equalize the bath-induced upward and downward transition rates in the qubit. By contrast, less frequent measurements conforming to the anti-Zeno (AZE) regime [8] predominantly enhance downward transitions (relaxation to the ground state) and thus are expected to purify ("cool") the qubit. These measurement-induced changes were predicted in Ref. [8] and go beyond previous studies that focused on transition-rate (relaxation) QZE-derived slowdowns and AZE-derived speedups [7] that have been experimentally verified [9].

This study considers a scenario different from that of Ref. [8]: the interaction of a spin-1/2 system S with N identical spin-1/2 particles I constituting its bath. This situation is encountered in NMR [5] and field-driven quantum dots [10]. Since all the I spins have the same energy levels, such spin baths are spectrally degenerate, as opposed to the broad spectrum of oscillator baths. The qubit-bath dynamics is therefore different for the two scenarios and hence we ask, do the equilibrium changes predicted in Ref. [8] hold in this case as well? This work demonstrates that they do: the purity of the system and bath spins can be lowered or raised via frequent induced dephasings that simulate QND energy measurements [7], by timing the dephasing intervals to be in the QZE (evolution slowdown) or AZE (evolution speedup) regime [7]. Repeated dephasings at intervals conforming to the AZE can in fact overcome even large frequency detunings of the qubit and bath spins, and induce polarization transfers that are comparable to those in a Hartmann-Hahn resonant transfer [11]. We term this novel effect as "incoherent resonance," as it stems from repeated erasures of the system-bath correlations.

Model and dynamical regimes.—The qubit-bath system will be described by the effective Hamiltonian

$$H = H_0 + H_{SI} + H_M(t). \qquad (1)$$

Here H_0 accounts for the coherent evolution of the qubit and bath, under a Zeeman-like interaction with respective Larmor frequencies ω_S and ω_I. H_{SI} couples the S and I spins, chosen to be oriented perpendicular to the Zeeman field,

$$H_{SI} = J\sum_k S^x I_k^x, \qquad (2)$$

S^x and I_k^x being Pauli operators. The time-dependent Hamiltonian $H_M(t)$ intermittently switches random fields that mimic repeated QND measurements.

The incoherent S-I cross-polarization transfer that we here discuss is determined by the interplay between "free" evolution and measurement effects, as follows.

(a) Free evolution: This is governed by the time-independent terms in Eq. (1). In the interaction picture, i.e., in a "doubly" rotating frame with frequencies ω_S and ω_I, H_{SI} has contributions from both rotating-wave (RW or

flip-flop) terms $S^+I_k^-$, oscillating as $e^{it(\omega_S-\omega_I)}$, and corotating (CR or flip-flip) terms $S^+I_k^+$ oscillating as $e^{it(\omega_S+\omega_I)}$, and by their respective Hermitian conjugate terms. The short-time evolution is dominated by the rapidly oscillating CR terms, and the long-time evolution by their RW counterparts. The energy transfer from I to S due to CR and RW terms is governed by the respective population transfer coefficients [12] $P_{CR} = \tilde{J}^2/[\tilde{J}^2 + (\omega_S + \omega_I)^2]$, $P_{RW} = \tilde{J}^2/[\tilde{J}^2 + (\omega_S - \omega_I)^2]$, where $\tilde{J}$ is the effective S-I interaction. At resonance ($\omega_S = \omega_I$), $P_{RW} = 1$, causing a complete exchange of polarization at $t \sim n\pi/J$ ($n = 1, 2, \dots$). In situations where $\omega_S, \omega_I > J$, one can ignore the fast-oscillating CR terms and obtain the dynamics using the RW terms only [11]. By contrast, under strongly mismatched conditions, e.g., $\omega_S \gg \omega_I$, $P_{RW} \sim P_{CR}$, and the dynamics is equally dominated by the CR and RW terms. For such large detunings, the H_{SI}-driven transfer of polarization between the S and I spins is inhibited: The polarizations of all spins are then locked at their initial values, as $P_{CR} \sim J/|\omega_S + \omega_I|$, $P_{RW} \sim J/|\omega_S - \omega_I| \ll 1$. While the presented results are focused on the given H_{SI}, they are general for Hamiltonians that contain RW and CR terms.

(b) *Projective measurements*: These will be imparted by brief interactions described by $H_M(t)$ [12]. Each such nonselective, projective measurement [8] erases the off-diagonal terms in the $S + I$ density matrix. This is equivalent to subjecting the system to a strong dephasing. Although the respective eigenstates of the system and the bath remain unchanged during these measurements, their correlation energy $\langle H_{SI} \rangle$ changes drastically, affecting subsequent evolution [8]. We mimic such projections onto the

system's energy eigenbasis by a NMR "quantum simulator," i.e., spatially random magnetic field gradients that change over time (see below).

The polarization exchange between the S, I spins is dramatically altered by these repeated projective measurements at times $n\tau$ ($n = 0, 1, 2, \dots$). We consider initially uncorrelated equilibrium states $\rho_S \otimes \rho_{I1} \otimes \cdots \otimes \rho_{IN}$, products of 2×2 density matrices of the S system and of the N I-bath spins that are diagonal in the energy eigenbasis, with populations of the excited spin state being $0 \leq \epsilon_{S(I)} \leq 1/2$ (their polarization $P_{S(I)} = 1 - 2\epsilon_{S(I)}$). $\epsilon_S(t)$ oscillates as the weighted sum (over all possible I-spin quantum numbers) of S-I oscillatory exchange probabilities. This function depends on N, the bath size, and on the anisotropy of the spin ensemble [12], but primarily on the time between consecutive dephasings: At short times $\omega_{S(I)}t \ll 1$, the S evolution is dominated by the fast-oscillating CR terms, so that the freely evolving polarization of the S spin is driven away from $[1 - 2\epsilon_S(0)]$, causing depolarization of S (heating): $\epsilon_S(t) < \epsilon_S(0)$. This CR heating is amplified by the repeated QZE, since CR evolution dominates under the QZE condition $(\omega_S + \omega_I)\tau \ll 1$ [12]: measurements or dephasing at intervals $\tau_h \lesssim 1/\sqrt{J^2 + (\omega_S + \omega_I)^2}$. This condition means that highly frequent measurements broaden the qubit levels to the extent that they become unresolved, equalizing upward and downward transition rates regardless of temperature [Fig. 1(a), red circles, and Fig. 1(b), lower inset]. By contrast, at longer intervals, the RW terms increase the polarization (cause cooling) of S: $\epsilon_S(t) > \epsilon_S(0)$. Such cooling, whose condition is $|\omega_S \pm \omega_I|\tau \gtrsim 1$, is amplified
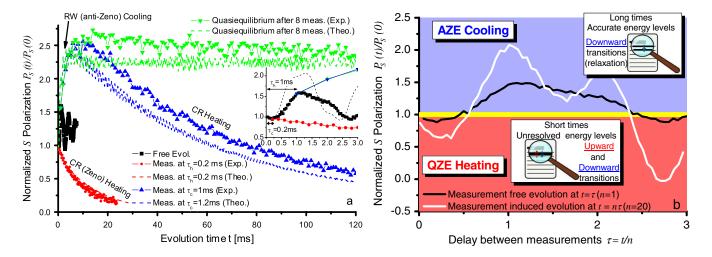

FIG. 1 (color online). Time evolution of the S-spin polarization. (a) The main panel compares S-spin polarization interrupted by repeated measurements at intervals of $\tau_c^{exp} = 1$ ms (blue upper triangles) and the evolution interrupted at $\tau_h = 0.2$ ms (red circles), respectively. A quasiequilibrium state is achieved for the τ_c^{exp} measurements, stopped after 8 ms and followed by free evolution at later times (green lower triangles). The S spin free evolution is shown with black squares. The inset zooms the dynamics for short times. The theoretical curves (dashed lines) are obtained by exact diagonalization of the Hamiltonian (1) for the experimental parameters above. (b) Schematic representation of the QZE and AZE in thermalized qubits. The white line is the S-spin quantum dynamics steered by $n = 20$ measurements upon varying the time interval τ. It evidences the predicted amplifications compared with the free evolution (black line). For short times (QZE regime), the levels are unresolved and their transition rates are equal (lower inset), while for long times (AZE regime) they are resolved and the downward transitions dominate (upper inset).

by the repeated AZE [8]: when measurements or dephasings happen at intervals $\tau_c \sim 1/\sqrt{J^2 + (\omega_S - \omega_I)^2}$, qubit levels are resolved and downward transitions dominate at finite temperature [Fig. 1(a), blue upper-triangles, and Fig. 1(b), upper inset]. Finally, after a few measurements (see below) the polarization transfer reaches close to the resonant maximum [$\epsilon_I(0)$] irrespective of the S-I detuning. These time scales determine a resonantlike characteristic that can be exploited as shown in Fig. 1. The qubit polarization is then described, within the RW domain, by Eq. (III.3) in the supplementary material [12].

(c) Quasiequilibrium: After a few measurements at suitable τ's, the polarization approaches an asymptotic value and the system reaches a quasiequilibrium state (see below), with polarization using RW terms only:

$$\epsilon_S^{qe} = \epsilon_S(0) + \frac{\epsilon_I(0) - \epsilon_S(0)}{2[1 - \epsilon_I(0)]}. \tag{3}$$

Depending on the sign of $\epsilon_I(0) - \epsilon_S(0)$, ϵ_S^{qe} can be either larger or smaller than $\epsilon_S(0)$, corresponding to S-spin cooling or heating, as compared to its initial equilibrium value. $(1 - 2\epsilon_S^{qe})$ is the largest obtainable polarization transfer from the I spins to the S spin, for any size N of the bath. The transfer achieved by the incoherent resonance is always greater than 50% of the coherent maximum, $\epsilon_I(0)/\epsilon_S(0)$, and bound by the full coherent maximum obtainable under a resonant transfer.

(d) Reheating: Once ϵ_S^{qe} is reached, the state of the total $(S + I)$ system commutes with the interaction Hamiltonian in the RW approximation, $[\rho, H_{SI}] \approx 0$. If no further measurements are performed, the evolution of all the spins is almost frozen [Fig. 1(a), green lower triangles]. Yet in a finite bath, as measurements continue to be performed, the deviations from Eq. (3) due to the CR terms gradually "reheat" (depolarize) both the S and the I spins [Fig. 1(b), blue upper triangles]. Hence, different desired quasiequilibrium values of the S polarization can be obtained depending on N, the bath size, and on the number of measurements performed beyond the number needed to attain ϵ_s^{qe}.

Results.—The foregoing predictions which hold for any size of the bath were tested by a liquid-state NMR simulator of QND measurement on ^{13}C-methyliodide (CH$_3$I) dissolved in CDCl$_3$. A ^{13}C spin (S) is J coupled to a finite bath of $N = 3$ equivalent ^{1}H spins (I) which interact with the S spin but not with each other. The quasiequilibrium value of polarization obtained for $N = 3$ is $\epsilon_S^{qe} = \epsilon_S(0) + \frac{1}{2}([\epsilon_I(0) - \epsilon_S(0)] \times \{1 + \epsilon_I(0)[1 - \epsilon_I(0)]\})$. The Hamiltonian (1) was reproduced by applying two rf fields on resonance with the respective I and S spins. In a doubly rotating frame we then obtain Hamiltonian (1) where the z axis is given by the rf field's direction and the frequencies ω_S and ω_I determined by the strength of the respective rf fields (see [12] for details). T_1 and T_2 relaxation times are assumed much longer than the time scales used for these quantum simulations.

To mimic the effects of projective measurements, we use pulsed magnetic field gradients. Field gradients effectively increase the decoherence rate for correlations in a plane
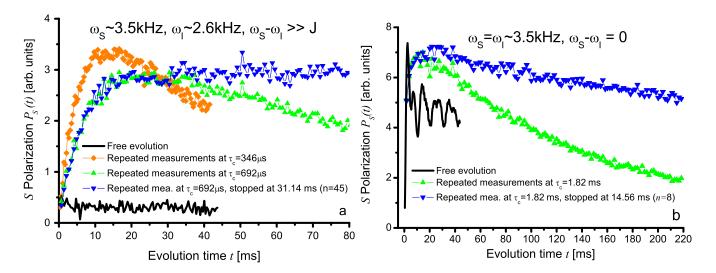

FIG. 2 (color online).   System polarization evolution under matching ($\omega_S = \omega_I$) and off-matching ($\omega_S \neq \omega_I$) conditions. (a) Free evolution (black solid line) of the system (S) spin polarization and its evolution interrupted by measurements at time intervals τ of 346 μs (orange circles) and 692 μs (green upper triangles) for off-resonant fields with high detuning. τ values were chosen to optimize the transfer. The quasiequilibrium state corresponding to measurements (at time intervals of 692 μs) stopped after 31.14 ms ($n = 45$), followed by the free evolution for the later times, is marked by blue lower triangles. (b) For resonant rf fields, we plotted the free evolution (black line) of S-spin polarization, interrupted by measurements at time intervals 1.82 ms (green upper triangle). The quasiequilibrium state corresponding to measurements (at time intervals of 1.82 ms) stopped after 14.56 ms ($n = 8$), followed by free evolution at later times, is marked by blue lower triangles. The maximal polarization transfer attained by resonant fields (black line) is almost the same as that achieved and maintained (blue lower triangles) by measurements for all later times.

perpendicular to the gradient's direction, which is along the B_0 field axis [13]. Since the repeated application of gradients can give origin to unwanted temporal correlations in the system's evolution [12], a sequence of dephasing operations that simulate projective measurements was implemented by applying at regular intervals random values of the field gradients [12]. In an ensemble average, the correlations are then effectively erased.

The initial conditions are $[1/2 - \epsilon_I(0)]/[1/2 - \epsilon_S(0)] \sim 4$ with the excitations $[1/2 - \epsilon_{I(S)}(0)] \ll 1$. By choosing the time intervals between measurements, to correspond to the QZE or AZE regimes, the depolarization (heating) or polarization (cooling) effects predicted by theory were indeed observed under nonmatching $\omega_I \sim 250$ Hz and $\omega_S \sim 420$ Hz [Fig. 1(a); $|\omega_S - \omega_I|, \omega_S, \omega_I \sim J = 150$ Hz enhances the predicted effects]. Additional measurements performed after attaining maximum polarization caused reheating of the S spin by CR terms, as predicted (blue upper triangles). Finally, by stopping the measurements after maximizing the polarization transfer, we observed the expected quasiequilibrium behavior of the S-spin (^{13}C) polarization (green lower triangles). Its value agrees well with the theoretically estimated $(1 - 2\epsilon_S^{qe}) \sim 2.9[1 - 2\epsilon_S(0)]$ considering only the RW term. Its slow decay is a consequence of nonideal pulses in the implementation of the projective measurements. Excellent agreement is evident between experimental results and numerical simulations without any fitting parameters. Figure 1(b) shows the experimental S polarization steered by $n = 20$ measurements as a function of their time interval τ. Heating (purity loss) or cooling (purity increase) depend on τ as predicted.

To further explore these incoherent polarization transfer effects, larger detunings $|\omega_S - \omega_I| \gg J$ ($\omega_S \sim 3.5$ kHz and $\omega_I \sim 2.6$ kHz) and fields $\omega_S, \omega_I \gg J$ were probed and compared with the Hartmann-Hahn resonant [11] transfer (Fig. 2). Only the I spins were initially excited while the S polarization was completely erased [$\epsilon_S(0) = 1/2$] [12], so that the actual polarization transferred from I to S spin could be determined. P_{RW} and P_{CR} were much lower than their resonant values, and the transfer arising from the free (uninterrupted) dynamics was negligible [Fig. 2(a), solid line]. By contrast, the $I \rightarrow S$ polarization transfer achieved by repeated projection measurements was unequivocally evidenced [Fig. 2(a)] to be close to the maximum achievable under resonant conditions [Fig. 2(b)].

Discussion.—The theoretical and experimental data in Figs. 1 and 2 demonstrate the connection between the fundamental Zeno and anti-Zeno effects in frequently measured or dephased open systems and their purity loss or increase, respectively. Measurement-induced transfer of polarization is then almost as effective as coherent on-resonance transfer, even if the measured system and bath are under presumably unfavorable, off-resonant conditions. We have further demonstrated the ability to steer

the system into a quasiequilibrium, which is maintained when further measurements are stopped. We envisage potential applications of this nonunitary polarization transfer protocol for qubit purification, required at the initialization stage of quantum information processing [14]. Increasing the polarization transfer from the pure I spins to the impure S spins even under off-resonant conditions could be useful for algorithmic cooling [15].

*Lucio.Frydman@weizmann.ac.il
†Gershon.Kurizki@weizmann.ac.il

[1] M. O. Scully *et al.*, Science **299**, 862 (2003).

[2] J. H. Wesenberg *et al.*, Phys. Rev. Lett. **103**, 070502 (2009).

[3] V. Giovannetti, S. Lloyd, and L. Maccone, Science **306**, 1330 (2004).

[4] L. Viola, E. Knill, and S. Lloyd, Phys. Rev. Lett. **82**, 2417 (1999); G. Gordon, G. Kurizki, and D. A. Lidar, Phys. Rev. Lett. **101**, 010403 (2008); A. Greilich *et al.*, Nature Phys. **5**, 262 (2009); J. Clausen, G. Bensky, and G. Kurizki, Phys. Rev. Lett. **104**, 040401 (2010); G. A. Álvarez and D. Suter, Phys. Rev. Lett. **104**, 230403 (2010); G. A. Álvarez *et al.*, Phys. Rev. A **81**, 060302(R) (2010).

[5] R. R. Ernst, G. Bodenhausen, and A. Wokaun, *Principles of Nuclear Magnetic Resonance in One and Two Dimensions* (Clarendon, Oxford, 1987).

[6] G. Gordon *et al.*, J. Phys. B **40**, S61 (2007); V. B. Braginsky and F. Ya. Khalili, Rev. Mod. Phys. **68**, 1 (1996).

[7] A. G. Kofman and G. Kurizki, Phys. Rev. Lett. **87**, 270405 (2001); Nature (London) **405**, 546 (2000); Phys. Rev. Lett. **93**, 130406 (2004).

[8] N. Erez *et al.*, Nature (London) **452**, 724 (2008); G. Gordon *et al.*, New J. Phys. **11**, 123025 (2009); G. Bensky *et al.*, Physica (Amsterdam) **42E**, 477 (2010).

[9] Q. Niu and M. G. Raizen, Phys. Rev. Lett. **80**, 3491 (1998); F. Dreisow *et al.*, Phys. Rev. Lett. **101**, 143602 (2008).

[10] P. Maletinsky, A. Badolato, and A. Imamoglu, Phys. Rev. Lett. **99**, 056804 (2007).

[11] S. R. Hartmann and E. L. Hahn, Phys. Rev. **128**, 2042 (1962).

[12] See supplementary material at http://link.aps.org/supplemental/10.1103/PhysRevLett.105.160401 for equation derivations, experimental procedures, and method justifications.

[13] L. Xiao and J. A. Jones, Phys. Lett. A **359**, 424 (2006).

[14] D. P. DiVincenzo, Fortschr. Phys. **48**, 771 (2000).

[15] J. Baugh *et al.*, Nature (London) **438**, 470 (2005).